Study of soft modes by temperature-derivative first- and second-order Raman spectroscopy

Y. Yacoby* and W. W. Kruhler
Max Planck Institut für Festkörperforschung, Stuttgart, Federal Republic, Germany

S. Just
Racach Institute of Physics, Hebrew University, Jerusalem, Israel
(Received 14 August 1975)

A study of soft modes in $SrTiO_3$ using a temperature-derivative Raman technique is reported. The A_{1g} component of the mode which softens towards the phase transition at 108 K has been studied below the phase-transition temperature. The energy of the modes as a function of temperature was followed down to 4 cm^{-1}. The square of the energy of this mode deviates from the Landau behavior for $T/T_c > 0.95$ and follows a temperature dependence very similar to that of the rotation of the octahedra in $SrTiO_3$. The soft ferroelectric mode has been observed for the first time in second-order Raman. It is shown that two structures in the spectra correspond to a replica of the soft mode and to the simultaneous emission of the soft mode and the absorption of an acoustic mode close to the Γ point.

I. INTRODUCTION

Since the discovery of the relation between the softening of certain vibrational modes and structural phase transitions by Cochran,[1,2] considerable attention has been given to the study of soft modes in crystals. Many systems have been studied so far and a comprehensive review of the subject has been given by Scott.[3] In recent years new discoveries were made regarding the behavior of crystals very close to their structural phase transition. Detailed EPR experiments on $SrTiO_3$ by Müller and Berlinger[4] have clearly shown for the first time that crystals which undergo a second-order structural phase transition also exhibit critical behavior. In the case of $SrTiO_3$ the order parameter was found to be the angle of rotation of the oxygen octahedra around a [100] axis. The dependence of $\langle\varphi\rangle$ on $(T_c - T)/T_c$ in $SrTiO_3$ and $LaAlO_3$ are almost exactly the same, showing that $\langle\varphi\rangle^2$ is indeed a valid order parameter in these systems. Outside the critical region $\langle\varphi\rangle^2$ is linear in $T_c' - T$ (for $T > 0.6T_c$), where T_c' is a temperature higher than the actual phase-transition temperature. Close to the phase-transition temperature, $\langle\varphi\rangle$ was found to be[4] proportional to $(T_c - T)^{\alpha}$, where $\alpha = 0.33 \pm 0.02$.

In 1970, Cowley[5] has proposed that in the neutron scattering spectrum one should observe in addition to the line corresponding to the soft mode also a central line corresponding to the elastic scattering of neutrons. This idea was further elaborated by Coombs and Cowley.[6] The intensity of this line should increase as the crystal approaches the phase-transition temperature both from above and from below. Moreover it was found that the frequency of the soft mode does not vanish at the phase transition. These discoveries had aroused a great deal of interest in the study of soft modes close to the phase-transition temperature. Fleury *et al.*[7] have measured the temperature dependence of both soft-mode components below the phase transition. In the range $0.5T_c < T < 0.9T_c$ the square of the soft-mode frequency was linear in $T_c - T$. Steigmeier and Auderset[8] have measured the frequency of the soft mode close to the phase-transition temperature, using Raman-scattering spectroscopy. Approaching the transition temperature from below they found that $\omega^2(T_c - T)$ deviates from linearity when $(T_c - T)/T_c > 0.9$. Owing to the intense laser light scattering at energies close to the laser-line frequency, they were not able to follow the peak of the soft mode to energies lower than $\omega = 15$ cm^{-1}. At this frequency, the deviation from linearity is still too small to be considered as proven beyond doubt.

The difficulty in studying soft modes close to the phase-transition temperature using Raman techniques arises primarily from the fact that the soft-mode line is often buried under the wings of the laser line. While the soft-mode frequency is strongly temperature dependent, the peak surrounding the laser line is in general much less temperature dependent. It is then quite obvious that a temperature-derivative Raman spectrum might be useful in studying soft modes.

In many materials the soft mode is not at the Brillouin-zone center. For example, above the transition temperature the soft mode of $SrTiO_3$ is at the R point. Using Raman spectroscopy, this mode can be observed only in second order. However, second-order Raman spectra are continuous, consequently it is difficult to obtain accurate information from such spectra. Wavelength-de-

rivative Raman spectroscopy[9] has improved the situation considerably. In these spectra one can directly measure the energies of pairs of phonons at Van Hove singularities and use the line shape to identify the experimental structures with particular points in the dispersion relations. Since soft modes are strongly temperature dependent, a temperature-derivative measurement of the Raman spectrum would enhance scattering processes associated with the soft mode compared to other scattering processes.

In this paper we report the first use of temperature-derivative Raman spectroscopy. We have applied this technique to the study of the soft A_{1g} mode below the structural-phase-transition temperature. We also observed for the first time second-order Raman scattering by the ferroelectric mode, and the ferroelectric mode was observed in two scattering processes: an overtone and the simultaneous emission of the ferroelectric phonon and the absorption of a TA phonon.

In Sec. II we discuss the experimental setup that was used to measure the temperature-derivative Raman spectra. In Sec. III we discuss first the theoretical line shapes one expects to find in temperature-derivative first-order Raman spectra. We then present the experimental spectra produced by the A_{1g} soft mode in $SrTiO_3$. These results are analyzed in comparison with the results of Müller and Berlinger[4] and of Shapiro *et al.*[10]

In Sec. IV we discuss the line shapes one expects to find in temperature-derivative second-order Raman spectra. The experimental results obtained in $SrTiO_3$ are then presented and interpreted. The properties of temperature-derivative Raman spectroscopy and the results of this work are summarized in Sec. V.

II. EXPERIMENTAL TECHNIQUE

The modulation of the temperature of the crystal was achieved using the setup shown in Fig. 1. To obtain sufficiently large temperature variations at a reasonable frequency, we have used crystals polished to a thickness of 100 μm. Small thickness is also important in maintaining the temperature uniformity throughout the scattering region. The sample was prepared in the following way: A thin film of Pt was evaporated on one face of the crystal. The surface electrical resistivity of the film was adjusted to 200 Ω; on both ends of the crystal we evaporated Al to form low-resistance contacts to the Pt film as shown in Fig. 1. We thus obtained 3×3-mm^2 resistive film. The crystal was mounted on a copper crystal holder, placing a $3\times3\times0.15$-mm^3 glass plate between the crystal and the copper. This plate was used as a thermal resistor.

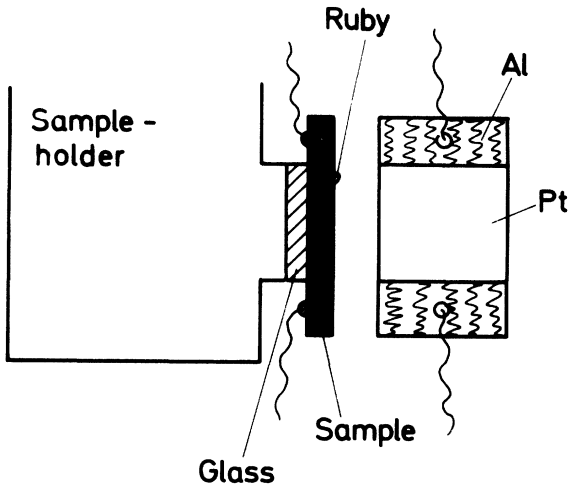

FIG. 1. Setup for the modulation of the temperature of crystalline samples.

The product of the heat capacity of the heated part of the crystal with the thermal resistance of the glass was chosen to be approximately $\frac{1}{6}$ sec so that the system will be best suited for a modulation frequency of 1 Hz.

The heater was connected to a square-wave voltage source with frequency of 1 Hz, riding on a dc level equal to one half of the peak-to-peak voltage. This produces a dc temperature change plus a 1-Hz ac temperature variation. The crystal is both heated and cooled on the *same side*, consequently the dc temperature of the crystal will be uniform throughout its thickness. On the other hand, there will be some nonuniformity in the ac component of the temperature; however, as it will be pointed out, this will not reduce the accuracy of our results.

The geometry of the measurement was as follows: The crystal was placed in a vertical position. Both top and bottom edges were optically polished. The laser light was applied through the bottom edge and the scattered light was collected through the film-free surface. We used an ordinary double spex monochrometer and a lock-in amplifier operating at 1 Hz. The sample was cooled down to the proper temperature in a continuous He flow Dewar. The temperature of the sample holder was measured by a Pt resistor and controlled to 0.1 K. At low temperatures a carbon resistor was used.

One of the main difficulties in this experiment is the precise measurement of the temperature of the sample itself. The dc temperature of the crystal differs from the temperature of the sample holder because of the dc and laser heating. In addition, it is necessary to measure the ac component of the temperature. Ordinary temperature measuring

devices such as a thermocouple cannot be used here because they affect the local thermal equilibrium leading to an erroneous temperature reading.

We first tried to use the resistivity change of a Pt film, but at these thicknesses the Pt resistivity is dominated by imperfections of the film rather than phonons; consequently, the resistivity is very insensitive to temperature changes. The method we finally used is as follows: We placed a tiny (less than 100 μm in diameter) lightly doped ruby crystal on the sample's surface. The ruby was small enough to thermalize with the sample in times shorter than 0.1 sec. We used part of the argon laser light to excite the $R1$ fluorescence line of the crystal. This line is very strong and sharp and its frequency is temperature dependent. This dependence has been very carefully established, both theoretically and experimentally.[11] We have used this property to measure the temperature shifts in the following way: The monochromator equipped with a wavelength-modulation device[9] is tuned to the peak of the line. The wavelength derivative of the fluorescence line, $dI_F/d\lambda$, is therefore zero. We now apply the argon laser to the crystal and put on the heater. As a result of the temperature change the $R1$ line is shifted and the derivative is no longer zero. We then adjust the spectrometer back to read a zero derivative value and measure the change in the $R1$ line frequency. Using the well-known dependence of the line frequency on temperature, we can then measure the temperature shift caused by the application of heat and of the laser light.

The main limiting factor in the determination of the temperature change by this method is the accurate measurement of the line shift. In our case this was limited by the mechanics of the monochrometer. To avoid this difficulty we have used a parallel glass plate placed behind the entrance slit. Rotation of this plate around an axis parallel to the slit, shifts the line. The shift is calibrated with respect to the changes in wavelength of the light transmitted by the monochrometer. In this way very small shifts in wavelength may be accurately measured.

The ac temperature component can also be measured by measuring the ac variation of $dI_F/d\lambda$ around its zero value and comparing the amplitude to the change in $dI_F/d\lambda$ associated with a known dc temperature change. Characteristic features of the system described above are as follows: The ac peak temperature change is approximately 0.25 K/mW. The dc temperature change is also approximately 0.25 K/mW. The accuracy in the measurement of the temperature changes (using the mechanical drive of the monochrometer) is 0.5 K; between 65 and 300 K; the accuracy is worse at lower temperatures because of the smaller shift of the line with temperature.

III. A_{1g} COMPONENT OF SOFT MODE IN $SrTiO_3$

In the cubic phase, $SrTiO_3$ has a soft mode at the R corner of the Brillouin zone. Its symmetry representation is Γ_{25}. This mode is, of course, Raman inactive in the first order. In the tetragonal phase, due to the doubling of the unit cell, the soft mode appears at the center of the Brillouin zone and therefore is Raman active in the first order. Moreover, the triply degenerate soft mode splits into a singly degenerate A_{1g} mode and a doubly degenerate E_g mode.

The line shapes theoretically expected in the temperature derivative Raman spectrum can be found by considering the Raman scattering tensor, taking anharmonic interaction into account. According to Cowley[12]

$$I^{(1)}_{\alpha\gamma\beta\lambda}(\Omega)=\frac{1}{2\pi}n(\Omega)\frac{4P^*_{\alpha\beta}P_{\gamma\lambda}\omega_0^2\Gamma}{(\omega_0^2+2\omega_0\Delta-\Omega^2)^2+4\omega_0^2\Gamma^2}. \quad (1)$$

Here Ω is positive for phonon absorption and negative for phonon emission; $n(\Omega)=|(e^{\beta\hbar\Omega}-1)^{-1}|$; $P_{\alpha\beta}$ is the polarizability tensor of a crystal perturbed by the long-wavelength vibrational mode $|Q(0,j)\rangle$, ω_0 is the self-energy of this mode in the harmonic approximation and is therefore temperature independent, and $\Pi=2\omega_0\Delta-2i\omega_0\Gamma$ is the self-energy correction. Δ and Γ are in general both temperature and frequency dependent. Expression (1) is not sufficient for the description of a system at temperatures very close to a second-order phase transition where the frequency of the mode approaches zero. In this case it is necessary to take into account another interaction channel which is important only at very low frequencies. The correction for the self-energy is given in this case in the form

$$\Pi=2\omega_0\Delta-2i\omega_0\Gamma-\gamma\delta^2/(\gamma-i\Omega). \quad (2)$$

Replacing this energy-correction term in Eq. (1) yields

$$I^{(1)}_{\alpha\gamma\beta\lambda}=(1/2\pi)n(\Omega)\frac{2P^*_{\alpha\beta}P_{\gamma\lambda}\omega_0[2\omega_0\Gamma+\delta^2\gamma\Omega/(\Omega^2+\gamma^2)]}{[\omega_\infty^2-\delta^2\gamma^2/(\Omega^2+\gamma^2)-\Omega^2]^2+[2\omega_0\Gamma+\delta^2\gamma\Omega/(\gamma^2+\Omega^2)]^2}. \quad (3)$$

Here $\omega_\infty^2 = \omega_0^2 + 2\omega_0\Delta$.

Shapiro *et al.*[10] have shown that this expression can be divided into a central component and a side component if $\omega_\infty^2 \gg \gamma^2$ and $\delta^2/\gamma \gg \Gamma$. The central component is given by

$$I^{(1)}_{\alpha\gamma\beta\lambda}(\Omega) = (2\pi)^{-1} n(\Omega) 2P^*_{\alpha\beta} P_{\gamma\lambda} \omega_0 \frac{\delta^2\Omega}{\omega_\infty^2 \omega_\infty'^2} \frac{\gamma'}{\Omega^2 + \gamma'^2}, \tag{4}$$

and the side component is given by

$$I^{(1)}_{\alpha\gamma\beta\lambda\ \text{side}}(\Omega) = (2\pi)^{-1} n(\Omega) 2P^*_{\alpha\beta} P_{\gamma\lambda} \omega_0 \frac{2\omega_0\Gamma}{(\omega_\infty^2 - \Omega^2)^2 + 4\omega_0^2\Gamma^2}. \tag{5}$$

Here $\omega_\infty'^2 = \omega_\infty^2 - \delta^2$ and $\gamma' = \gamma\omega_\infty'^2/\omega_\infty^2$.

The central part of the scattering tensor gives rise to a peak at $\Omega = 0$ with a width of γ', whereas the side component gives rise to a structure with a peak at $\omega = \omega_\infty$ and width equal to $2\omega_0\Gamma$. Evidence from neutron scattering[13] at temperatures above the phase transition show that $\gamma' < 5\times10^{-3}$ cm^{-1}. Thus, in our experiments it is expected that only the side scattering component would be observed, however the tail of the central component may show up at small Ω through the finite resolutions of the spectrometer. The total intensity of scattered light is proportional to $(\omega_\infty'^2)^{-1}$ and is expected to diverge at the phase transition temperature. Thus $\omega_\infty'^2$ vanishes at this temperature, but ω_∞^2 remains finite.

The temperature derivative of the side component of the scattering tensor is given by

$$\frac{dI^{(1)}_{\text{side}}}{dT} = I^{(1)}\left[n^{-1}(\Omega)\frac{dn(\Omega)}{dT} - 2\frac{d\omega_\infty^2}{dT}\frac{\omega_\infty^2 - \Omega^2}{(\omega_\infty^2 - \Omega^2)^2 + 4\omega_0^2\Gamma^2} + \frac{d(\omega_0\Gamma)}{dT}(2\omega_0\Gamma)^{-1} \times\left(1 - \frac{8\omega_0^2\Gamma^2}{(\omega_\infty^2 - \Omega^2)^2 + 4\omega_0^2\Gamma^2}\right)\right]. \tag{6}$$

The temperature derivative of the scattered intensity is therefore divisible into three parts: The first is associated with the change of the Planck occupation number $n(\Omega)$. The spectral shape of the component is similar to that of $I^{(1)}(\Omega)$ and is schematically shown in Fig. 2(a). The second is associated with the shift of the frequency ω_∞^2 with temperature. The line shape of this component is shown in Fig. 2(b). The third component results from the change of the broadening parameter $\omega_0\Gamma$ and it gives rise to a line of the form shown in Fig. 2(c).

The temperature derivative spectra of first-order Raman scattering produced by the A_{1g} mode were measured in $SrTiO_3$ under the following conditions: (a) The scattering configuration was $z[x,(z,x)]Y$. In this configuration all three species A_{1g}, E_g, and T_{2g} may contribute to the spectrum. However, no information has been lost in this case because the A_{1g} mode contributes only to the A_{1g} species. We preferred to use unpolarized scattered light in order to improve our signal-to-noise ratio. (b) The amplitude of the temperature variation ΔT was kept as low as possible. The spectra presented below were measured with $\Delta T = 0.5$ K. (c) The laser intensity was kept down to 200 mW and was slightly defocused to avoid local laser heating. (d) After every dc temperature change we waited for 2 h before measuring the spectrum. (e) The monochromator slit widths were 250 μm for $T < 0.97T_c$ and 150 μm for $T > 0.97T_c$.

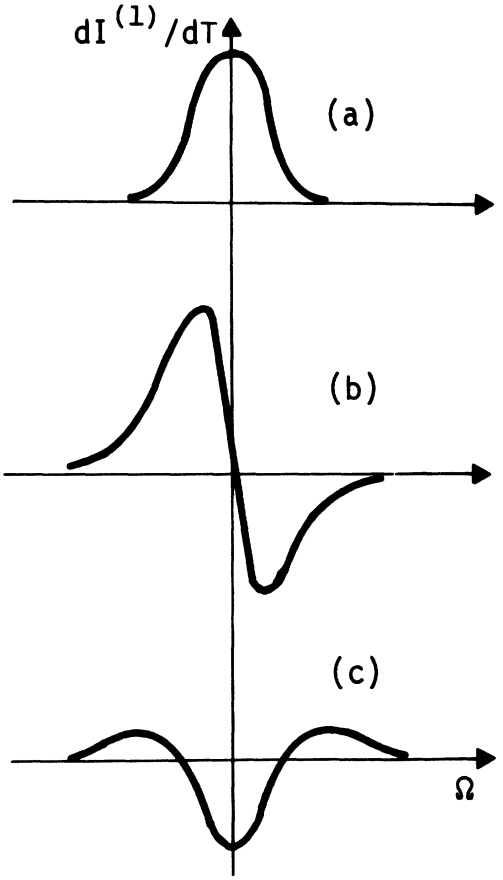

FIG. 2. Schematic line shapes of temperature-derivative first-order Raman spectra.

Five examples of the temperature derivative first-order Raman spectrum produced by the soft A_{1g} mode are shown in Fig. 3. Several features should be noticed: (a) The spectra have the form of the wavelength derivative of a Lorenzian. (b)

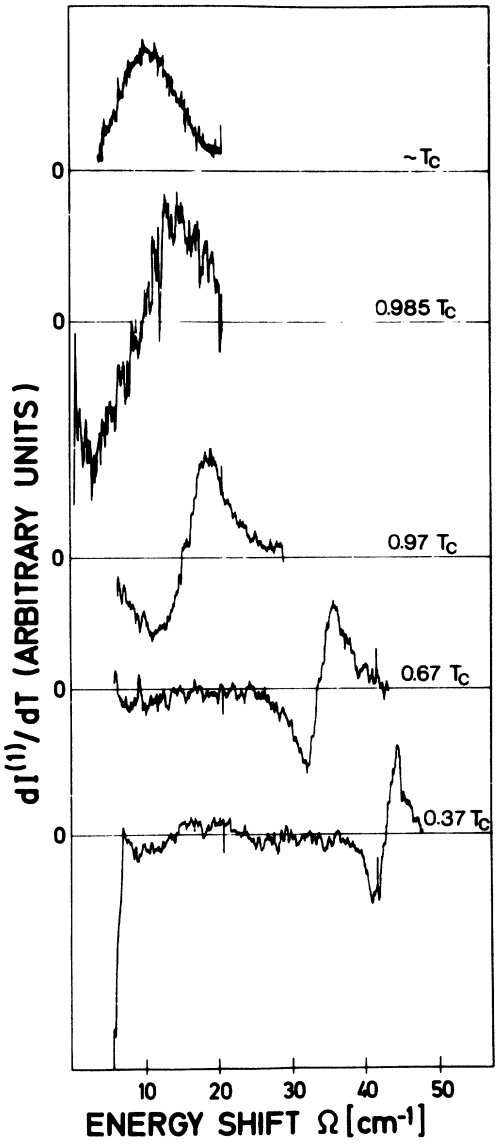

FIG. 3. Examples of temperature-derivative first-order Raman spectra produced by the A_{1g} mode of $SrTiO_3$.

The linewidth clearly increases as the phase transition is approached. (c) The spectrum at $\sim T_c$ was measured down to 3.75 cm^{-1} from the laser line. The spectrum could not be followed below this energy because of excessive noise. Comparison of the experimental line shapes with the line-shape components shown in Fig. 2 indicates that the second component, produced by the change in the mode frequency with temperature, is completely dominant. This result appears to be somewhat surprising in view of the fact that the linewidth does change very significantly. However, inspection of the second component of $dI^{(1)}/dT$ reveals that the linewidth is indeed expected to change even for $\omega_0\Gamma$ constant if ω_∞^2 changes. We observe that

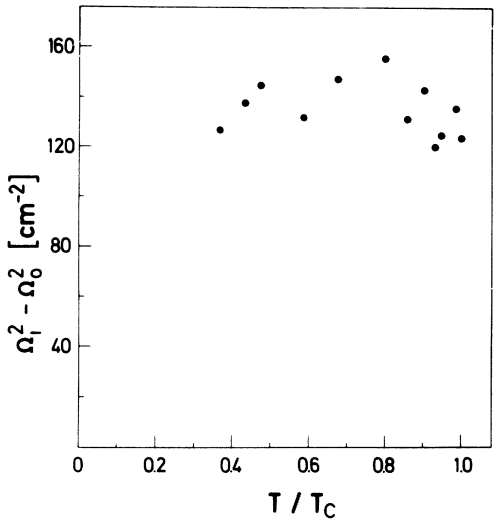

FIG. 4. $4\omega_0^2\Gamma^2$ as a function of temperature.

$$4\omega_0^2\Gamma^2 = \Omega_1^2 - \Omega_0^2, \tag{7}$$

where Ω_1 and Ω_0 are frequencies for which the second component in Eq. (6) has maximum and zero values, respectively.

In Fig. 4 we plot $\Omega_1^2 - \Omega_0^2$ as a function of temperature. Indeed the experimental results show that $\Omega_1^2 - \Omega_0^2$ remains constant within the experimental accuracy. The numerical value of this constant is $4\omega_0^2\Gamma^2 = 140\ cm^{-2}$.

Let us now consider the temperature dependence of ω_∞^2. Inspection of Eq. (6) shows that if the second component is dominant, ω_∞^2 is determined by the zero points in the $dI^{(1)}/dT$ spectra. The temperature dependence of ω_∞^2 is shown in Fig. 5. The results clearly show a deviation from the Landau behavior both at low temperatures $T < 0.6T_c$ and for high temperature $0.95T_c < T < T_c$. On the same plot we also present the temperature dependence of the octahedron rotation angles squared $\langle\varphi^2\rangle$. In comparing the two curves we adjusted the phase transition temperature in both curves and the values of $\langle\varphi\rangle^2$ and of ω_∞^2 at one other temperature. The two curves are identical within the experimental accuracy for $0.6T_c < T < T_c$ except for one point. At $T = T_c$, $\varphi = 0$ whereas $\omega_\infty \neq 0$. As was pointed out, this is to be expected, because at the phase transition $\omega_\infty' = 0$. Measurements of ω_∞ by Shapiro *et al.*[10] also show that ω_∞ does not vanish at the phase-transition temperature but saturates at $\sim 4.7\ cm^{-1}$. This value is in rough agreement with the lowest value we could measure. The temperature dependence of ω_∞^2 definitely deviates from linearity for temperatures $0.95T_c < T$

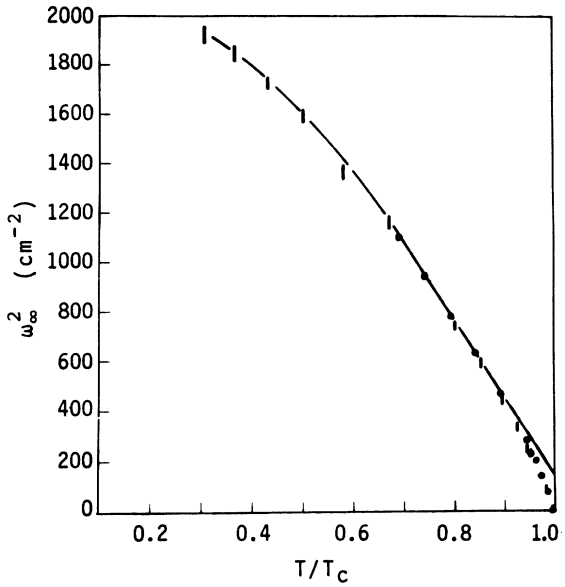

FIG. 5. ω_∞^2 as a function of T/T_c. Vertical bars indicate the experimental results. The size of the bars indicate the experimental uncertainty. Also shown are the values of $\langle\varphi\rangle$ indicated by dots. These are taken from the results of Müller and Berlinger (Ref. 4).

$< T_c$. The exact temperature dependence in this temperature range could not be determined yet, with safety, because T_c was not determined independently. If we use the value obtained for T_c by Müller and Berlinger,[4] the experimental values follow a $(T_c - T)^{1/3}$ law. However, the actual exponent is very sensitive to the critical temperature. Thus this result cannot be regarded at this point as well established.

Outside the critical region the molecular-field approximation would be valid. It is therefore expected that the relation, between the frequency of the soft A_{1g} mode below the transition and the soft mode above the transition,[14] would hold, namely

$$\omega^2_{A_{1g}}(T_c - \Delta T) = 2\omega_R^2(T_c + \Delta T) . \tag{8}$$

Experimentally, the slope of the linear portion of $\omega^2_{A_{1g}}$ measured in our results is 29.2 cm^{-2}/K. The slope of ω_R^2 in Shapiro *et al.*[10] results for $T > T_c$ is 13.37 cm^{-2}/K. The ratio between the slopes is 2.18 which is within 10% from the predicted value.

IV. TEMPERATURE-DERIVATIVE SECOND-ORDER RAMAN SCATTERING INVOLVING FERROELECTRIC MODE

The scattering tensor of a second-order Raman process may be expressed as follows:

$$I^{(2)}(\Omega) = \sum_{\vec{K}} n(\omega_1)n(\omega_2)I_0(\vec{K}) \times \delta[\Omega - \omega_1(\vec{K}) - \omega_2(\vec{K})]. \tag{9}$$

In this expression ω_1 and ω_2 are dependent on the crystal momentum $\vec{K}$. They are positive for phonon absorption and negative for phonon emission. $I_0(\vec{K})$ is the contribution to the scattering tensor by two normal vibrational modes with frequencies ω_1 and ω_2 and crystal momentum equal to $\vec{K}$ or $-\vec{K}$. (Phonon-phonon and phonon-impurity scattering processes have been neglected.) Every one of the terms in the above expression is momentum and frequency dependent. However, in a crude way the expression in Eq. (9) may be regarded as the product of the scattering tensor produced by a pair of phonons $n(\omega_1)n(\omega_2)I_0(\vec{K})$ multiplied by the density of states

$$\rho(\Omega) = \sum_{\vec{K}} \delta[\Omega - \omega_1(\vec{K}) - \omega_2(\vec{K})] .$$

The strongest frequency dependence is found near energies known as the Van Hove critical energies. These energies are defined through the requirement that $\vec{\nabla}_{\vec{K}}[\omega_1(\vec{K}) + \omega_2(\vec{K})] = 0$. At these points the density of states has a discontinuous wavelength derivative. The behavior of second-order Raman scattering in the vicinity of such points has been extensively discussed.[15] Temperature affects the spectrum of the scattered light in two ways. It changes the temperature in the expression for $n(\omega_1)$ and $n(\omega_2)$ and it also changes ω_1 and ω_2 for a given $\vec{K}$ value. Thus we may divide $dI^{(2)}(\Omega)/dT$ into two parts:

$$\frac{dI^{(2)}(\Omega)}{dT} = \sum_{\vec{K}} \delta[\Omega - \omega_1(\vec{K}) - \omega_2(\vec{K})]\frac{d}{dT}[n(\omega_1)n(\omega_2)I_0(\vec{K})] + \sum_{\vec{K}} n(\omega_1)n(\omega_2)I_0(\vec{K})\frac{d}{dT}\delta[\Omega - \omega_1(\vec{K}) - \omega_2(\vec{K})] . \tag{10}$$

The first term in this expression is continuous in frequency. In a crude way this term represents the change in the scattering produced by a pair of phonons without changing the density of states. Consequently its spectral form would be similar to that of $I^{(2)}(\Omega)$. On the other hand, the second term is crudely the product of the scattering tensor of a pair of phonons and the temperature derivative of the density of states.

In the vicinity of a Van Hove singularity,

$$\frac{d}{dT}\sum_{\vec{K}} \delta[\Omega - \omega_1(\vec{K}) - \omega_2(\vec{K})] = -\left(\frac{d}{dT}[\omega_1(\vec{K}_c) + \omega_2(K_c)]\right) \times \frac{d}{d\Omega}\sum_{\vec{K}} \delta[\Omega - \omega_1(\vec{K}) - \omega_2(\vec{K})] , \tag{11}$$

namely the temperature derivative is proportional

to the wavelength derivative of the density of states. The line shapes appearing in wavelength-derivative Raman spectra in the vicinity of Van Hove singularities has been extensively discussed.[15] Neglecting broadening effects, the lines have singularities at the Van Hove critical energies. Thus, the main contribution to the temperature derivative spectrum is expected to arise from the second term in Eq. (10).

The ordinary spectrum of second-order Raman scattering of $SrTiO_3$ has been experimentally studied.[16] However, its interpretation was rather crude and little information has been extracted from it. In particular, no evidence has been found to the contribution of soft modes to this spectrum. The frequency of two modes is known to vary strongly with temperature: the Γ_{25} mode at R and the TO_1 (ferroelectric mode) at the zone center. In the present study we have measured the spectra of $dI^{(2)}/dT$ at different temperatures. Three examples of these spectra are shown in Fig. 6. The spectra were taken in a $Z[X,(X,Z)]Y$ configuration with an ac temperature amplitude of $\Delta T = 4$ K. Measuring time of the spectra was about 4 h. The long measuring times were necessary to obtain sufficiently large signal-to-noise ratio. It is interesting to note several features of these spectra: (a) both peaks shift very significantly to higher energies with temperature. This might be expected from the fact that they appear in a temperature derivative spectrum. (b) The linewidths of the peaks increases very significantly as the temperature is raised. (c) The spectra shown in Fig. 6 are very different from the ordinary Raman spectra. Both peaks appear also in the wavelength-derivative Raman spectra among other structures which are not strongly temperature dependent.[16] From this we may conclude that peaks A and B are caused primarily by the frequency change, namely, they correspond to the second term in Eq. (10).

Moreover, from Fig. 6 we observe that $d(\omega_1 + \omega_2)/dT > 0$. Since $dI^{(2)}/dT < 0$, we conclude from Eq. (11) that $d\rho(\Omega)/d\Omega > 0$. Structures A and B therefore correspond to scattering from either a minimum (m_0) or a saddle point (m_1) in the phonon dispersion relations.

In Fig. 7 we plot the frequency of peak B, ω_B and half of the frequency of peak A, $\frac{1}{2}\omega_A$, as a function of temperature. ($\frac{1}{2}\omega_A$ was chosen for reasons of interpretation). Note that both frequencies increase with increasing temperature in a rather similar way. The spacing between the two curves also increases with temperature. Comparison of

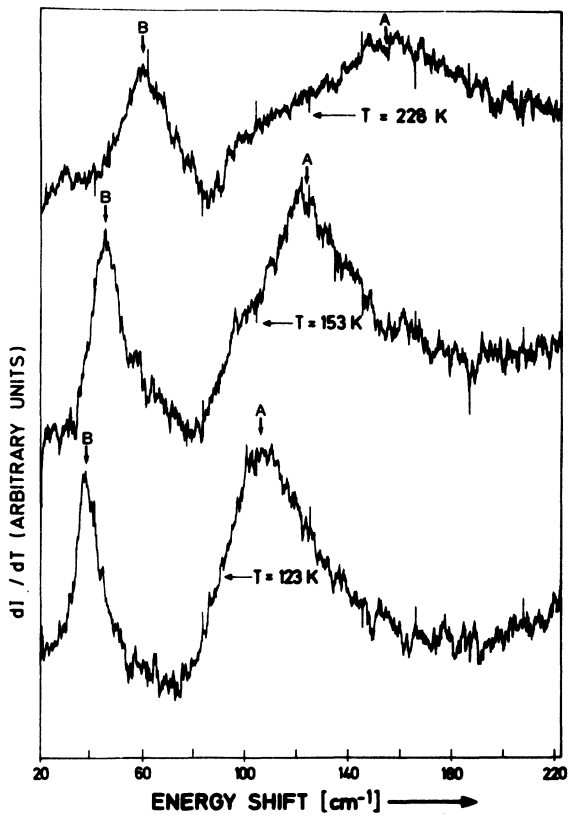

FIG. 6. Examples of temperature-derivative second-order Raman spectra of $SrTiO_3$.

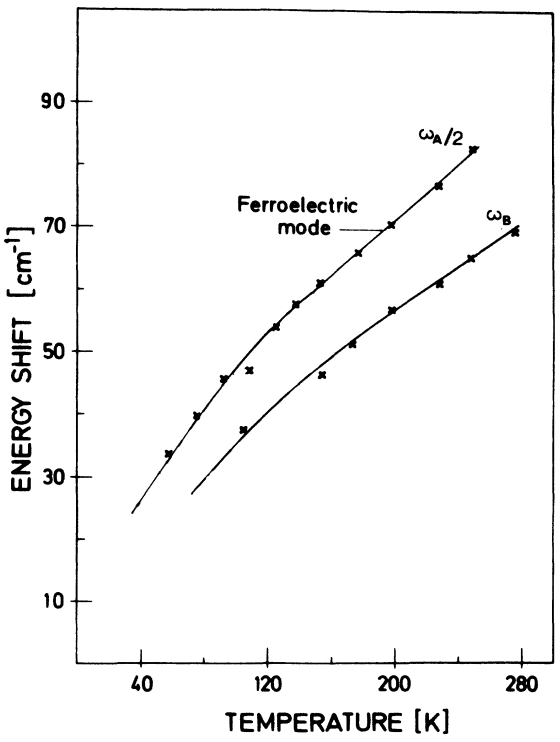

FIG. 7. Temperature dependence of $\frac{1}{2}\omega_A$ and ω_B.

the results presented in Fig. 7 with the results of Fleury and Worlock[17] for the temperature dependence of the ferroelectric mode, shows that $\frac{1}{2}\omega_A$ is equal to the ferroelectric mode energy. This mode has indeed a minimum at Γ.

The interpretation of line B is less obvious. Line B can be observed down to very low temperatures. Thus it can either be associated with the simultaneous emission of two phonons or with the emission of one and the absorption of another with small energy. The energy of the absorbed phonon should not exceed 30 cm^{-1} at low temperatures. In the case of the emission of two phonons, one phonon should have an energy less than 15 cm^{-1}. Inspection of the dispersion relations given by Stirling[18] shows that there is no combination of two emitted phonons that could explain line B. The only process which can account for line B is the emission of the ferroelectric mode and the absorption of an accoustic mode.

The energy difference between the TO_1 mode and the TA mode has a minimum at a point which lies on the [100] direction. The energy difference between the TO_1 (ferroelectric mode) and the LA mode has also a minimum but the energy difference at this minimum is in complete disagreement with our experimental value at room temperature. Second-order Raman scattering involving the TO_1 and the TA modes along [100] are allowed in all three species A_{1g}, E_g, and T_{2g}. Both $A_{1g} + E_g$ and T_{2g} were observed. This interpretation naturally explains the temperature dependence of line B. It also explains the sign of the observed peak.

It is interesting to note that the difference $\omega_A/2 - \omega_B$ is also temperature dependent. This quantity should have been constant if the curvature of $\omega_{TO_1}(\vec{K})$ did not change with temperature. This curvature is known to increase with decreasing temperature and it is easily observed that this would cause $\omega_A/2 - \omega_B$ to increase with temperature. This effect is indeed observed in Fig. 7.

The results presented in Fig. 7 can be more thoroughly understood by analyzing small-$\vec{K}$ vector phonons in terms of the zone-center phonons. The vibration of any atom ln in the direction i associated with a vibrational mode $|Q(\vec{K},j))$ may be expressed in the form $(lni\,|\,Q(\vec{K},j)) = (ni\,|\,\tilde{Q}(\vec{K},j))\, e^{i\vec{k}\cdot\vec{l}}$, where $\vec{l}$ is the unit-cell vector, n the number of the atom in the unit cell, and $|\tilde{Q}(\vec{K},j))$ is the periodic part of the eigenvector. At any point $\vec{K}$, the eigenvectors $|\tilde{Q}(\vec{K},j))$ form a complete set such that $|\tilde{Q}(\vec{K},j)) = \Sigma_{j'} a_{jj'}\,|\tilde{Q}(\vec{K},j))$. Following Axe *et al.*[19] we may now express the TO_1 and TA vibrational modes at small $\vec{K}$ in terms of the phonons at $\vec{K}=0$. Since the energy difference between TO_1 and TA is small at low temperatures, we assume that $a_{jj'}$ would involve only these modes. $a_{jj'}$ satisfies then the following equation:

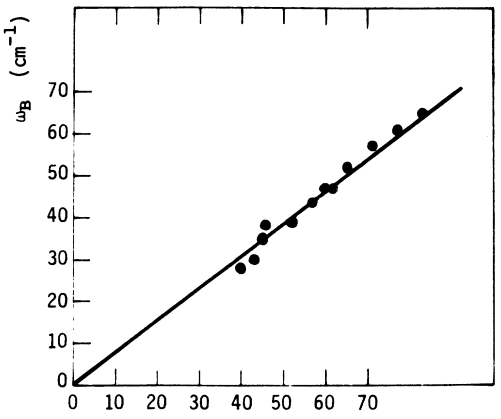

FIG. 8. ω_B as a function of $\frac{1}{2}\omega_A$.

$$\begin{pmatrix} \omega_0^2 + Y_{11} & Y_{12} \\ Y_{12} & Y_{22} \end{pmatrix} \begin{pmatrix} a_{1j} \\ a_{2j} \end{pmatrix} = \omega_j^2(\vec{K}) \begin{pmatrix} a_{1j} \\ a_{2j} \end{pmatrix}. \quad (12)$$

In this expression Y_{11}, Y_{12}, and Y_{22} are even functions of $\vec{K}$ and $\omega_0 = \omega_{TO}(\vec{K}=0)$. Equation (12) can be solved if

$$\begin{vmatrix} \omega_0^2 + Y_{11} - \omega_j^2(\vec{K}) & Y_{12} \\ Y_{12} & Y_{22} - \omega_j^2(\vec{K}) \end{vmatrix} = 0. \quad (13)$$

This equation then yields the energies of the TO_1 and TA modes at small values of $\vec{K}$. Both solutions are functions of $\vec{K}$ and ω_0. If we assume that Y_{11}, Y_{12}, and Y_{22} are proportional to K^2, then

$$\omega_j(t\vec{K}, t\omega_0) = t\,\omega_j(\vec{K}, \omega_0) \quad \text{for any } t\,.$$

Thus, it is easily observed that if

$$\vec{\nabla}_{\vec{K}}[\omega_{TO_1}(\vec{K}, \omega_0) - \omega_{TA}(\vec{K}, \omega_0)] = 0 \quad \text{for } \vec{K} = \vec{K}_0\,,$$

then

$$\vec{\nabla}_{\vec{K}}[\omega_{TO_1}(\vec{K}, t\omega_0) - \omega_{TA}(\vec{K}, t\omega_0)] = 0 \quad \text{for } \vec{K} = t\vec{K}_0\,.$$

This leads us to the final result that the frequency difference $\omega_{TO_1}(\vec{K}_0, \omega_0) - \omega_{TA}(\vec{K}_0, \omega_0)$, evaluated at the point $\vec{K}_0$, where the gradient of this frequency difference vanishes, is proportional to ω_0.

In Fig. 8 we plot the energy difference $\omega_B = \omega_{TO_1} - \omega_{TA}$ as a function of $\frac{1}{2}\omega_A = \omega_0$. It is observed that the two are indeed linearly dependent. The ratio $(\omega_{TO_1} - \omega_A)/\omega_0$ can be expressed in terms of $Y_{11}^{(0)}$, $Y_{12}^{(0)}$, and $Y_{22}^{(0)}$ as follows:

$$[\omega_{TO_1}(K_0\omega_0) - \omega_{TA}(K_0\omega_0)]^2/\omega_0^2$$

$$= 1 + \frac{Y_{22}^{(0)}}{2D}(Y_{11}^{(0)} + Y_{22}^{(0)} - 2\sqrt{D}) \times \left[\left(\frac{Y_{11}^{(0)2} + 2Y_{12}^{(0)2} + Y_{22}^{(0)2} + 2D}{Y_{11}^{(0)2} + 2Y_{12}^{(0)2} + Y_{22}^{(0)2} - D}\right)^{1/2} - 1\right], \quad (14)$$

where $D = Y_{11}^{(0)}Y_{22}^{(0)} - Y_{12}^{(0)2}$, $Y_{11} = Y_{11}^{(0)}K^2$, $Y_{12} = Y_{12}^{(0)}K^2$, and $Y_{22} = Y_{22}^{(0)}K^2$.
The numerical value of this ratio can be found from Fig. 8 and is equal to $2\omega_B/\omega_A = 0.77$.

V. SUMMARY

In this paper we have presented the first application of temperature-derivative Raman spectroscopy to the study of soft modes. The main advantage of this method stems from its ability to enhance processes originating in soft modes as compared to other scattering processes. The modulation of temperature is achieved by using small enough crystals and carefully matching the thermal RC constant to the frequency of modulation. This match is important in order to decrease the power needed for the modulation and the dc temperature rise accompanying it. The main difficulty in the technique is the accurate measurement of the temperature of the sample itself. This was achieved by using the temperature dependence of the $R1$ line of ruby crystals.

Using this technique, it was possible to follow the A_{1g} component of the soft mode down to 3.75 cm^{-1}. This enabled us to observe a clear deviation from the Landau predicted behavior. The temperature dependence of ω_∞^2 for temperatures between 0.6 T_c and T_c fits very well the temperature dependence of $\langle\varphi\rangle^2$ measured by Müller and Berlinger. However, this agreement was obtained by fitting the phase-transition temperature in the two curves. It would be necessary to perform an independent measurement of the transition temperature simultaneously with the Raman measurement in order to determine accurately the critical dependence of ω_∞^2 on temperature. Temperature derivative second-order Raman spectra of $SrTiO_3$ showed two structures; one was interpreted as the overtone of the ferroelectric mode. The other was attributed to scattering involving the simultaneous emission of the ferroelectric mode and the absorption of a TA mode along the [100] direction at a point where the energy difference between the two is at minimum. This interpretation predicts that the ratio between the energies of the two peaks would be constant. This is indeed experimentally verified.

In conclusion, temperature derivative Raman spectroscopy can be expected to be useful in a variety of problems involving strongly temperature-dependent excitations such as vibrational modes and magnons, both at the center of the Brillouin zone and at other points.

---

*Present adress: Racach Institute of Physics, Hebrew University, Jerusalem, Israel.

[1]W. Cochran, Adv. Phys. 9, 387 (1960).
[2]W. Cochran, Adv. Phys. 10, 401 (1961).
[3]J. F. Scott, Rev. Mod. Phys. 46, 83 (1974).
[4]K. A. Müller and W. Berlinger, Phys. Rev. Lett. 26, 13, (1971).
[5]R. A. Cowley, J. Phys. Soc. Jpn. Suppl. 28, 239 (1970).
[6]G. J. Coombs and R. A. Cowley, J. Phys. (Paris) C Suppl. 33, 57 (1972); G. J. Coombs and R. A. Cowley, J. Phys. C 6, 121, (1973); R. A. Cowley and G. J. Coombs, *ibid.* 6, 143 (1973).
[7]P. A. Fleury, J. F. Scott, and J. M. Worlock, Phys. Rev. Lett. 21, 16 (1968).
[8]E. F. Steigmeier and H. Auderset, Solid State Commun. 12, 565 (1973).
[9]Y. Yacoby and A. Linz, Phys. Rev. B 9, 2723 (1974).
[10]S. M. Shapiro, J. D. Axe, and G. Shirane, Phys. Rev. B 6, 4332 (1972).
[11]D. G. McCumber and M. D. Sturge, J. Appl. Phys. 34, 1682 (1963).
[12]R. A. Cowley, Proc. Phys. Soc. Lond. 84, 281, (1964).
[13]S. Töpler, B. Alefeld, and A. Kollmar, Phys. Lett. A 51, 297 (1975).
[14]H. Thomas and K. A. Müller, Phys. Rev. Lett. 21, 1256 (1968).
[15]Y. Yacoby *Optical Properties of Solids, New Developments*, edited by B. O. Seraphin (North-Holland, Amsterdam, 1975).
[16]Y. Yacoby and W. W. Kruhler (unpublished).
[17]P. A. Fleury and J. M. Worlock, Phys. Rev. 174, 613 (1968).
[18]W. G. Stirling, J. Phys. C 5, 2711 (1972).
[19]J. D. Axe, J. Harada, and G. Shirane, Phys. Rev. B 1, 1227 (1970).